The Unscented Kalman Filter and Particle Filter Methods for Nonlinear Structural System Identification with Non-Collocated Heterogeneous Sensing[‡]

Eleni N. Chatzi*[†] and Andrew W. Smyth [§]

Department of Civil Engineering & Engineering Mechanics, Columbia University, New York, NY 10027, USA

SUMMARY

The use of heterogeneous, non-collocated measurements for non-linear structural system identification is explored herein. In particular, this paper considers the example of sensor heterogeneity arising from the fact that both acceleration and displacement are measured at various locations of the structural system. The availability of non-collocated data might often arise in the identification of systems where the displacement data may be provided through Global Positioning Systems (GPS). The well known Extended Kalman Filter (EKF) is often used to deal with nonlinear system identification. However, as suggested in [1], the EKF is not effective in the case of highly nonlinear problems. Instead, two techniques are examined herein, the Unscented Kalman Filter method (UKF), proposed by Julier and Uhlman, and the Particle Filter method, also known as Sequential Monte Carlo method (SMC). The two methods are compared and their efficiency is evaluated through the example of a three degree of freedom system, involving a Bouc Wen hysteretic component, where the availability of displacement and acceleration measurements for different DOFs is assumed.

KEY WORDS: Non-Linear System Identification, Unscented Kalman Filter, Particle Filter, Heterogeneous Sensing

*Correspondence to: Eleni N. Chatzi, Department of Civil Engineering & Engineering Mechanics, Columbia University, New York, NY 10027, USA.
[†]PhD Candidate, email: ec2451@columbia.edu
[§]Associate Professor, email: smyth@civil.columbia.edu
[‡]Presented in the International Symposium on Structural Control and Health Monitoring, National Chung Hsing University, Taichung, Taiwan, ROC, January 10-11, 2008

1. INTRODUCTION

In the past two decades there has been great interest in the efficient simulation and identification of nonlinear structural system behavior. The availability of acceleration and often also displacement response measurements is essential for the effective monitoring of structural response and the determination of the parameters governing it. Displacement and/or strain information in particular is of great importance when it comes to permanent deformations.

The availability of acceleration data is usually ensured since this is what is commonly measured. However, most nonlinear models are functions of displacement and velocity and hence the convenience of acquiring access to those signals becomes evident. In practice, velocities and displacements can be acquired by integrating the accelerations although the latter technique presents some drawbacks. The recent advances in technology have provided us with new methods of obtaining accurate position information, through Global Position System (GPS) receivers for instance. In this paper the potential of exploiting combined displacement and acceleration information for different degrees of freedom of a structure (non-collocated, heterogeneous measurements) is explored. Also, the influence of displacement data availability is investigated in section 5.3.

The nonlinearity of the problem (both in the dynamics and in the measurement equations as will be shown) requires the use of sophisticated computational tools. Many techniques have been proposed for nonlinear applications in Civil Engineering, including the Least Squares Estimation (LSE) [1], [2], the extended Kalman Filter (EKF) [3], [4], [5], the Unscented Kalman Filter (UKF) [6], [7] and the Sequential Monte Carlo Methods (Particle Filters) [8], [9], [10], [11]. The adaptive least squares estimation schemes depend on measured data from the structural system response. Since velocity and displacement are not often readily available, for their implementation these signals have to be obtained by integration and/or differentiation schemes. As mentioned above, this poses difficulties associated with the noise component in the signals.

The EKF has been the standard Bayesian state-estimation algorithm for nonlinear systems for the last 30 years and has been applied over a number of civil engineering applications such as structural damage identification [12], parameter identification of inelastic structures [13] and so on. Despite its wide use, the EKF is only reliable for systems that are almost linear on the time scale of the updating intervals. The main concept of the EKF is the propagation of a Gaussian Random variable (GRV) which approximates the state through the first order linearization of the state transition and observation matrices of the nonlinear system, through Taylor series expansion. Therefore, the degree of accuracy of the EKF relies on the validity of the linear approximation and is not suitable for highly non-Gaussian conditional probability density functions (PDFs) due to the fact that it only updates the first two moments.

The UKF, on the other hand does not require the calculation of Jacobians (in order to linearize the state equations). Instead, the state is again approximated by a GRV which is now represented by a set of carefully chosen points. These sample points completely capture the true mean and covariance of the GRV and when propagated through the actual nonlinear system they capture the posterior mean and covariance accurately to the second order for any nonlinearity (third order for Gaussian inputs) [7]. The UKF appears to be superior to the EKF especially for higher order nonlinearities as are often encountered in civil engineering problems. Mariani and Ghisi have demonstrated this for the case of softening single degree-of-freedom systems [14] and Wu and Smyth show that the UKF produces better state estimation and parameter identification than the EKF and is also more robust to measurement noise levels for higher degree of freedom systems [15].

The Sequential Monte Carlo Methods (particle filters) can deal with nonlinear systems with non Gaussian posterior probability of the state, where it is often desirable to propagate the conditional PDF itself. The concept of the method is that the approximation of the posterior probability of the state is done through the generation of a large number of samples (weighted particles), using Monte Carlo Methods. Particle Filters are essentially an extension to point-mass filters with the difference that the particles are no longer uniformly distributed over the state but instead concentrate in regions of high probability. The basic drawback is the fact that depending on the problem a large number of samples may be required thus making the PF analysis computationally expensive.

In this paper we will apply both the UKF and the Particle Filter methods for the case of a three degree of freedom structural identification example, which includes a Bouc Wen hysteretic element which leads to increased nonlinearity. In the next sections a brief review of each method is presented in the context of nonlinear state space equations.

2. THE GENERAL PROBLEM AND THE OPTIMAL BAYESIAN SOLUTION

Consider the general dynamical system described by the following nonlinear continuous state space (process) equation

$$\dot{x} = f(x(t)) + v(t) \tag{1}$$

and the nonlinear observation equation at time $t = k\Delta t$

$$y_k = h(x_k) + \eta_k \tag{2}$$

where x_k is the state variable vector at $t = k\Delta t$, $v(t)$ is the zero mean process noise vector with covariance matrix $Q(t)$. y_k is the zero mean observation vector at $t = k\Delta t$ and η_k is the observation noise vector with corresponding covariance matrix R_k. In discrete time, equation (1) can be rewritten as follows so that we obtain the following discrete nonlinear state space equation:

$$x_{k+1} = F(x_k) + v_k \tag{3}$$

$$y_k = h(x_k) + \eta_k \tag{4}$$

where v_k is the process noise vector with covariance matrix Q_k, and function F is obtained from equation (1) via integration:

$$F(x_k) = x_k + \int_{k\Delta t}^{(k+1)\Delta t} f(x(t))dt \tag{5}$$

From a Bayesian perspective the problem of determining filtered estimates of x_k based on the sequence of all available measurements up to time k, $y_{1:k}$ is to recursively quantify the efficiency of the estimate, taking different values. For that purpose, the construction of a posterior PDF is required $p(x_k|y_{1:k})$. Assuming the prior distribution $p(x_0)$ is known and that the required PDF $p(x_{k-1}|y_{1:k-1})$ at time $k-1$ is available, the prior probability $p(x_k|y_{1:k-1})$ can be obtained sequentially through prediction (Chapman-Kolmogorov Equation for the predictive distribution):

$$p(x_k|y_{1:k-1}) = \int p(x_k|x_{k-1})p(x_{k-1}|y_{1:k-1})dx_{k-1} \tag{6}$$

The probabilistic model of the state evolution $p(x_k|x_{k-1})$, also referred to as transitional density, is defined by the process equation (3) (i.e., it is fully defined by $F(x_k)$ and the process noise distribution $p(v_k)$). Consequently, the prior (or prediction) is updated using the measurement y_k at time k, as follows (Bayes Theorem):

$$p(x_k|y_{1:k}) = p(x_k|y_k, y_{1:k-1}) = \frac{p(y_k|x_k)p(x_k|y_{1:k-1})}{p(y_k|y_{1:k-1})} \tag{7}$$

where the normalizing constant $p(y_k|y_{1:k-1})$ depends on the likelihood function $p(y_k|x_k)$ defined by the observation equation (4),(i.e., it is fully defined by $h(x_k)$ and the observation noise distribution $p(\eta_k)$).

The recurrence relations (6), (7) form the basis of the optimal Bayesian solution. Once the posterior PDF is known the optimal estimate can be computed using different criteria, one of

which is minimum mean square error (MMSE) estimate which is the conditional mean of x_k:

$$E\{x_k|y_{1:k}\} = \int x_k \cdot p(x_k|y_{1:k})dx_k \tag{8}$$

or otherwise the maximum a posteriori (MAP) estimate can be used which is the maximum of $p(x_k|y_{1:k})$.

However, since the Bayesian solution is hard to compute analytically we have to resort to approximations or suboptimal Bayesian algorithms such as the ones described below.

3. THE UNSCENTED KALMAN FILTER

The UKF approximates the posterior density $p(x_k|y_{1:k})$ by a Gaussian density, which is represented by a set of deterministically chosen points. The UKF relates to the Bayesian approach equations (6), (7) presented above through the following recursive relationships:

$$\begin{aligned} p(x_{k-1}|y_{1:k-1}) &= N(x_{k-1}; \hat{x}_{k-1|k-1}, P_{k-1|k-1}) \\ p(x_k|y_{1:k-1}) &= N(x_k; \hat{x}_{k|k-1}, P_{k|k-1}) \\ p(x_k|y_{1:k}) &= N(x_k; \hat{x}_{k|k}, P_{k|k}) \end{aligned} \tag{9}$$

where $N(x; m, P)$ is a Gaussian density with argument x, mean m and covariance P.

More specifically, given the state vector at step $k-1$ and assuming that this has a mean value of $\hat{x}_{k-1|k-1}$ and covariance $p_{k-1|k-1}$, we can calculate the statistics of x_k by using the Unscented Transformation, or in other words by computing the sigma points χ_k^i with corresponding weights W_i. For further details, one can refer to [15] and [16]. These sigma points are propagated through the nonlinear function $F(x_k)$:

$$\chi_{k|k-1}^i = F(\chi_{k-1}^i), i = 0, .., 2L \tag{10}$$

where L is the dimension of the state vector x.

The set of the sample points $\chi_{k|k-1}^i$ represents the predicted density $p(x_k|y_{1:k-1})$. Then the mean and covariance of the next state are approximated using a weighted sample mean and covariance of the posterior sigma points and the time update step is continued as follows:

$$\hat{x}_{k|k-1} = \sum_{i=0}^{2L} W_i^{(m)} \chi_{k|k-1}^i \tag{11}$$

$$P_{k|k-1} = \sum_{i=0}^{2L} W_i^{(c)} [\chi_{k|k-1}^i - \hat{x}_{k|k-1}][\chi_{k|k-1}^i - \hat{x}_{k|k-1}]^T + Q_{k-1} \tag{12}$$

The predicted measurement is then equal to:

$$\hat{y}_{k|k-1} = \sum_{i=0}^{2L} W_i^{(m)} h(\chi_{k|k-1}^i) \tag{13}$$

Then the measurement update equations are as follows:

$$\hat{x}_{k|k} = \hat{x}_{k|k-1} + K_k(y_k - \hat{y}_{k|k-1}) \tag{14}$$

$$P_{k|k} = P_{k|k-1} - K_k P_k^{YY} K_k^T \tag{15}$$

where

$$K_k = P_k^{XY}(P_k^{YY} - R_k)^{-1} \tag{16}$$

$$P_k^{YY} = \sum_{i=0}^{2L} W_i^{(c)} [h(\chi_{k|k-1}^i) - \hat{y}_{k|k-1}][h(\chi_{k|k-1}^i) - \hat{y}_{k|k-1}]^T + R_k \tag{17}$$

$$P_k^{XY} = \sum_{i=0}^{2L} W_i^{(c)} [\chi_{k|k-1}^i - \hat{x}_{k|k-1}][h(\chi_{k|k-1}^i) - \hat{y}_{k|k-1}]^T \tag{18}$$

where K_k is the Kalman gain matrix at step k.

4. THE PARTICLE FILTER

In this section a general overview of the Particle Filtering techniques will be provided. The key idea of these methods is to represent the required posterior probability density function (PDF) by a set of random samples with associated weights and to compute estimates based on these. As the number of samples increases this Monte Carlo approach becomes an equivalent representation of the function description of the PDF and the solution approaches the optimal Bayesian estimate.

Particle Filters approximate the posterior PDF $p(x_k|y_{1:k})$ by a set of support points $x_k^i, i = 1, ..., N$ with associated weights w_k^i. The importance weights are decided using importance sampling [17], [18]. In essence the standard Particle Filter method is a modification of the Sequential Importance Sampling method along with a Re-sampling step. Importance sampling is a general technique for estimating the properties of a particular distribution, while

only having samples generated from a different distribution rather than the distribution of interest [19], [20]. Suppose we can generate samples from a density $q(x)$ which is similar to $p(x)$, meaning that:

$$p(x) > 0 \Rightarrow q(x) > 0 \; \forall x \tag{19}$$

Then any integral of the form $I = \int p(x)dx$ can be written as $I = \int \frac{p(x)}{q(x)} w(x)dx$, provided that $p(x)/q(x)$ is upper bounded. Then a Monte Carlo estimate is computed drawing N independent samples from $q(x)$ and forming the weighted sum:

$$I_N = \frac{1}{N} \sum_{i=1}^{N} w_k^i \delta(x_k - x_k^i) \; where \; w_k^i = \frac{p(x^i)}{q(x^i)} \tag{20}$$

where $\delta(x)$ is the Dirac delta measure. This means that the probability density function at time k can be approximated as follows:

$$p(x_k|y_{1:k}) = \sum_{i=1}^{N} w_k^i \delta(x_k - x_k^i) \tag{21}$$

where

$$w_k^i \propto \frac{p(x_k^i|y_{1:k})}{q(x_k^i|y_{1:k})} \tag{22}$$

where x_k^i are the N samples drawn at time step k from the importance density function $q(x_k^i|y_{1:k})$ which will be defined later. The weights are normalized so that their sum is equal to unity. Using the state space assumptions (1st order Markov / observational independence given state), the importance weights can be estimated recursively by [proof in De Freitas (2000)]:

$$w_k^i \propto w_{k-1}^i \frac{p(y_k|x_k^i)p(x_k^i|x_{k-1}^i)}{q(x_k^i|x_{k-1}^i, y_k)} \tag{23}$$

where $p(x_k^i|x_{k-1}^i)$ is the transitional density, defined by the process equation (3) and $p(y_k|x_k)$ is the likelihood function defined by the observation equation (4).

A common problem that is connected to the implementation of Particle Filters is that of degeneracy, meaning that after some time steps significant weight is concentrated on only one particle, thus considerable computational effort is spent on updating particles with negligible contribution to the approximation of $p(x_k|y_{1:k})$. A measure of degeneracy is the following estimate of the effective sample size:

$$N_{eff} = \frac{1}{\sum_{i-1}^{N_s} (w_k^i)^2} \tag{24}$$

Re-sampling is a technique aiming at the elimination of degeneracy. It discards those particles with negligible weights and enhances the ones with larger weights (usually duplicates large weight samples). Re-sampling takes place when N_{eff} falls below some user defined threshold N_T. Re-sampling is performed by the generation of a new set $x_k^{i*}{}_{i=1}^{N}$ which occurs by replacement from the original set [21], so that $Pr(x_k^{i*} = x_k^j) = w_k^j$. The weights are in this way reset to $w_k^i = 1/N$ and therefore become uniform. This is schematically shown in Figure 1.

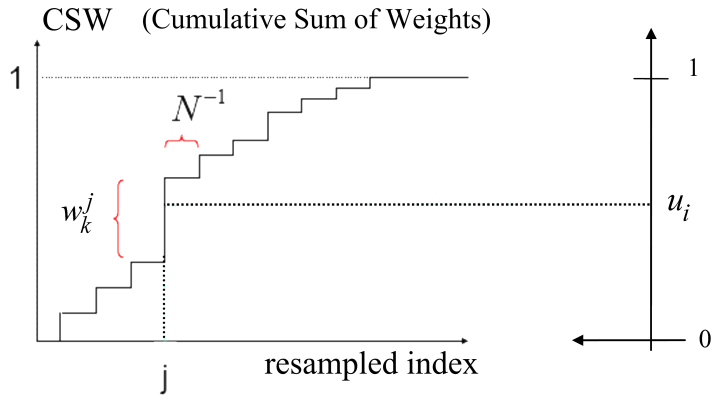

Figure 1. The process of Re-sampling: the random variable u_i uniformly distributed in [0,1], maps into index j, thus the corresponding particle x_k^j is likely to be selected due to its considerable weight w_k^j

The use of the Re-sampling technique however may lead to other problems. As the high weight particles are selected multiple times, diversity amongst particles is not maintained. This phenomenon known as sample impoverishment [10] (or particle depletion), is most likely to occur in the case of small process noise. Known techniques for tackling the sample impoverishment problem include the use of crossover operators from genetic algorithms are adopted to tackle the finite particle problem by re-defining or re-supplying impoverished particles during filter iterations [22], the use of SVR based re-weighting schemes [23], or the application of the Expectation Maximization algorithm which is further described in section 4.1 of this paper.

A second issue in the implementation of Particle Filters is the selection of the importance density. It has been proved that the optimal importance density function that minimizes the

variance of the true weights is given by:

$$q(x_k|x_{k-1}^i, y_{1:k})_{opt} = p(x_k|x_{k-1}^i, y_k) = \frac{p(y_k|x_k, x_{k-1}^i)p(x_k|x_{k-1}^i)}{p(y_k|x_{k-1}^i)} \tag{25}$$

However, sampling from $p(x_k|x_{k-1}^i, y_k)$ might not be straightforward, leading to the use of the transitional prior as the importance density function:

$$q(x_k|x_{k-1}^i, y_{1:k}) = p(x_k|x_{k-1}^i) \tag{26}$$

which from equation (23) yields:

$$w_k^i = w_{k-1}^i p(y_k|x_k^i) \tag{27}$$

This means that at time step k the samples x_k^i are drawn from the transitional density, which is actually totally defined by the process equation (3). Also, the selection of the importance weights is essentially dependent on the likelihood of the error between the estimate and the actual measurement as this is defined by equation (4). Alternatively, a Likelihood based importance density function can be used [10], or even a suboptimal deterministic algorithm [21].

Particle Filters present the advantage that as the number of particles approaches infinity, the state estimation converges to its expected value and also parallel computations are possible for PF algorithms. On the other hand an increased number of particles unavoidably means a significant computational cost which can be a major disadvantage. It should be noted however that the UKF also provides the potential for parallel computing and is in itself a considerably faster tool than the PF technique.

4.1. Particle Filtering Methods Used

In the example presented next, two different particle filter techniques were utilized, namely the Generic PF (or Bootstrap Filter of Condensation) and the Sigma Point Bayes Filter. The Generic Particle Filter described earlier can be summarized by the following steps which are graphically presented in Figure 2.

a) Draw samples from the importance density IS (usually the transitional prior) -Predict.

b) Evaluate the importance weights based on the likelihood function -Measure.

c) Re-sample if the effective number of particles is below some threshold and normalize weights -Re-sample.

d) Approximate the posterior PDF through the set of weighted particles.

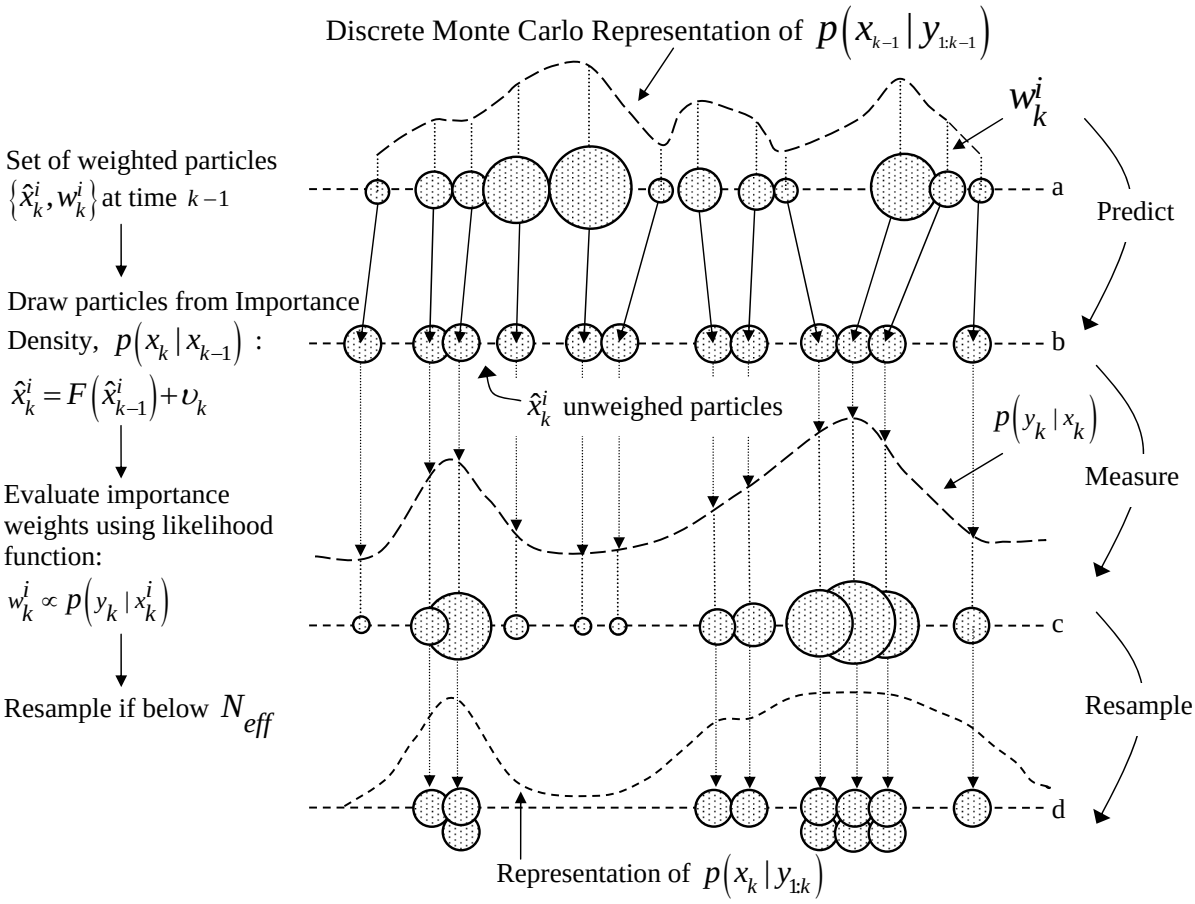

Figure 2. Generic Particle Filter Algorithm Outline:a) Predict, b) Measure, c)Re-sample, d) Approximate the posterior pdf

The second PF method applied in this paper is the Sigma Point Bayes Filter or Gaussian Mixture Sigma-Point Particle Filter (GMSPPF), which is an extension of the original "Unscented Particle Filter" of Van der Merwe, De Freitas and Doucet. The GMSPPF combines an importance sampling (IS) based measurement update step with a Sigma Point Kalman Filter (Square Root Unscented KF - SRUKF or Square Root Central Difference KF - SRCDKF) for the time update and importance density generation. More explicitly, the time update step involves the approximation of the posterior density of step $k-1$ by a G-component Gaussian Mixture Model (GMM) of the following form:

$$p_G(x) = \sum_{g=1}^{G} \alpha^{(g)} N(x; m^{(g)}, P^{(g)}) \tag{28}$$

where G is the number of mixing components, $\alpha^{(g)}$ are the mixing weights and $N(x; m, P)$ is a normal distribution with mean vector m and positive definite covariance matrix P. Similar GMM models are used for the modeling of the process and observation densities. Next, for each one of the components of the GMM a Sigma Point Kalman Filter (SPKF) time update step takes place followed by a measurement update step for each SPKF, using equation (4) and the current observation. Then, the predictive state density $p_G(x_k|y_{1:k-1})$ and the posterior state density $p_G(x_k|y_{1:k})$ are approximated as GMMs. The posterior state density will be used as the proposal distribution for the measurement update step.

The measurement update step initiates with by drawing N samples from the aforementioned proposal distribution. The corresponding weights are calculated and normalized as described in detail in [19]. A weighted Expectation Maximization (EM) algorithm is then used in order to fit the G-component GMM to the set of N weighted particles that represent the approximate posterior distribution at time k, i.e. $p_G(x_k|y_{1:k})$. The EM step replaces the standard Re-sampling technique used in the Generic Particle Filter, thus mitigating the sample depletion problem. The Expectation Maximization algorithm recovers a maximum likelihood GMM fit to the set of weighted samples, leading to both the smoothing of the posterior set (and the avoidance of the sample impoverishment problem) and the use of a reduced number of mixing components in the posterior, leading to a lower computational cost. The pseudo code for the GMSPPF can be found in [19].

5. APPLICATION: DUAL STATE AND PARAMETER ESTIMATION FOR A 3 - MASS DAMPED SYSTEM

The model utilized in the particular example is presented in figure 3.

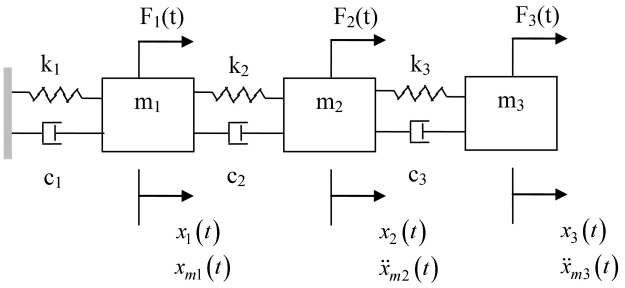

Figure 3. Model of the 3-DOF system example. Note that the first degree of freedom is associated with a non- linear hysteretic component

The objective is to determine the "clean" displacement values along with the parameters of the system given displacement measurements (GPS) for m_1 and accelerometer measurements for m_2 and m_3. Also, the first DOF is assumed to have a degrading hysteretic behavior described by Bouc-Wen's formula. The state space equations governing the system can be formulated as follows:

$$\underset{\sim}{x} = \begin{bmatrix} x_1 \\ x_2 \\ x_3 \end{bmatrix} \rightarrow \begin{bmatrix} m_1 & 0 & 0 \\ 0 & m_2 & 0 \\ 0 & 0 & m_3 \end{bmatrix} \begin{bmatrix} \ddot{x}_1 \\ \ddot{x}_2 \\ \ddot{x}_3 \end{bmatrix} + \begin{bmatrix} c_1 + c_2 & -c_2 & 0 \\ -c_2 & c_2 + c_3 & -c_3 \\ 0 & -c_3 & c_3 \end{bmatrix} \begin{bmatrix} \dot{x}_1 \\ \dot{x}_2 \\ \dot{x}_3 \end{bmatrix} + \\ + \begin{bmatrix} k_1 & k_2 & -k_2 & 0 \\ 0 & -k_2 & k_2 + k_3 & -k_3 \\ 0 & 0 & -k_3 & k_3 \end{bmatrix} \begin{bmatrix} r_1 \\ x_1 \\ x_2 \\ x_3 \end{bmatrix} = \begin{bmatrix} F_1(t) \\ F_2(t) \\ F_3(t) \end{bmatrix} \tag{29}$$

where $r_1(t)$ is the Bouc - Wen hysteretic component with:

$$\dot{r}_1(t) = \dot{x}_1 - \beta |\dot{x}_1| |r_1|^{n-1} r - \gamma (\dot{x}_1) |r_1|^n \tag{30}$$

β, γ, n are the Bouc-Wen hysteretic parameters which will also be identified.

Combining the equations of motion (29) into the classic state space formulation (where $x_1, \ddot{x}_2, \ddot{x_3}$ are the measured quantities) and assuming that the state vector is augmented

to include the system parameters $(k_i, c_i, \beta, \gamma, n)$ as variables we can obtain the following formulation:

$$\begin{bmatrix} \dot{z}_1 \\ \dot{z}_2 \\ \dot{z}_3 \\ \dot{z}_4 \\ \dot{z}_5 \\ \dot{z}_6 \\ \dot{z}_7 \\ \dot{z}_8 \\ \dot{z}_9 \\ \dot{z}_{10} \\ \dot{z}_{11} \\ \dot{z}_{12} \\ \dot{z}_{13} \\ \dot{z}_{14} \\ \dot{z}_{15} \\ \dot{z}_{16} \end{bmatrix} = \begin{bmatrix} \dot{x}_1 \\ \dot{x}_2 \\ \dot{x}_3 \\ \dot{r}_1 \\ \ddot{x}_1 \\ \ddot{x}_2 \\ \ddot{x}_3 \\ \dot{k}_1 \\ \dot{k}_2 \\ \dot{k}_3 \\ \dot{c}_1 \\ \dot{c}_2 \\ \dot{c}_3 \\ \dot{\beta} \\ \dot{\gamma} \\ \dot{n} \end{bmatrix} = \begin{bmatrix} z_5 \\ z_6 \\ z_7 \\ (z_5 - z_{14}\left|z_5\right|\left|z_4\right|^{z_{16}-1} z_4 + \\ -z_{15} z_5 \left|z_4\right|^{z_{16}}) \\ (-z_8 \cdot z_4 - z_9 \cdot z_1 + z_9 \cdot z_2 + \\ -(z_{11} + z_{12}) \cdot z_5 + z_{12} \cdot z_6)/m_1 \\ 0 \\ 0 \\ 0 \\ 0 \\ 0 \\ 0 \\ 0 \\ 0 \\ 0 \\ 0 \\ 0 \\ 0 \end{bmatrix} + \begin{bmatrix} 0 \\ 0 \\ 0 \\ 0 \\ \upsilon_1 + \frac{F_1(t)}{m_1} \\ \ddot{x}_{m2} + \upsilon_2 \\ \ddot{x}_{m3} + \upsilon_3 \\ 0 \\ 0 \\ 0 \\ 0 \\ 0 \\ 0 \\ 0 \\ 0 \\ 0 \end{bmatrix} \tag{31}$$

$$y = \begin{bmatrix} x_{m1} \\ \ddot{x}_{m2} \\ \ddot{x}_{m3} \end{bmatrix} = \begin{bmatrix} 1 & 0 & 0 & 0 & 0 & 0 \\ k_2/m_2 & -\frac{k_2+k_3}{m_2} & k_3/m_2 & c_2/m_2 & -\frac{c_2+c_3}{m_2} & c_3/m_2 \\ 0 & k_3/m_3 & -k_3/m_3 & 0 & c_3/m_3 & -c_3/m_3 \end{bmatrix} \begin{bmatrix} x_1 \\ x_2 \\ x_3 \\ \dot{x}_1 \\ \dot{x}_2 \\ \dot{x}_3 \end{bmatrix} + \begin{bmatrix} \eta_1 \\ \eta_2 \\ \eta_3 \end{bmatrix} + \begin{bmatrix} 0 \\ F_2(t)/m_2 \\ F_3(t)/m_3 \end{bmatrix} \tag{32}$$

Equations (31), (32) can be compactly written in matrix form as:

$$\begin{aligned} \dot{z} &= A(z) + \ddot{x}_m + \upsilon + F_a \\ y &= H(z) + \eta + F_d \end{aligned} \tag{33}$$

where,

A, H are non-linear functions of the state variables.
z is the state variable vector:
$z = [\ x_1 \quad x_2 \quad x_3 \quad r_1 \quad \dot{x}_1 \quad \dot{x}_2 \quad \dot{x}_3 \quad k_1 \quad k_2 \quad k_3 \quad c_1 \quad c_2 \quad c_3 \quad \beta \quad \gamma \quad n\ ]^T$.
y is the observation vector.
$\ddot{x}_m$ are the acceleration measurements.
υ is the process noise vector.
η is the observation noise vector.
F_a, F_d are the excitation vectors corresponding to the process and observation equations respectively.

The system equation is nonlinear not only due to the presence of the bilinear terms involving state components, such as $z_8 \cdot z_4$ etc, but also due to the use of one of the equilibrium equations in the process equation for $\ddot{x}_1$ and (30) for $\dot{r}_1$ which makes the particular problem highly non-linear. The transformation into discrete time now becomes (where acceleration is measured in intervals of T):

$$\begin{bmatrix} z_{1(k+1)} \\ z_{2(k+1)} \\ z_{3(k+1)} \\ z_{4(k+1)} \\ z_{5(k+1)} \\ z_{6(k+1)} \\ z_{7(k+1)} \\ z_{8(k+1)} \\ \vdots \\ z_{16(k+1)} \end{bmatrix} = \begin{bmatrix} z_{1(k)} + T z_{5(k)} \\ z_{2(k)} + T z_{6(k)} \\ z_{3(k)} + T z_{7(k)} \\ z_{4(k)} + T \left\{ \begin{array}{c} z_{5(k)} - z_{14(k)} \left| z_{5(k)} \right| \left| z_{4(k)} \right|^{z_{16(k)-1}} \\ + z_{4(k)} - z_{15(k)} z_{5(k)} \left| z_{4(k)} \right|^{z_{16(k)}} \end{array} \right\} \\ z_{5(k)} + \frac{T}{m_1} \left\{ \begin{array}{c} -z_{8(k)} z_{4(k)} - z_{9(k)} \left(z_{1(k)} - z_{2(k)} \right) \\ -\left(z_{11(k)} + z_{12(k)} \right) z_{5(k)} + z_{12} z_{6(k)} \end{array} \right\} \\ z_{6(k)} \\ z_{7(k)} \\ z_{8(k)} \\ \vdots \\ z_{16(k)} \end{bmatrix} + \begin{bmatrix} 0 \\ 0 \\ 0 \\ 0 \\ T\upsilon_1 + T\frac{F_{1(k)}}{m_1} \\ T\ddot{x}_{m2(k)} + T\upsilon_2 \\ T\ddot{x}_{m3(k)} + T\upsilon_3 \\ 0 \\ \vdots \\ 0 \end{bmatrix} \tag{34}$$

$$\begin{bmatrix} x_{m1(k)} \\ \ddot{x}_{m2(k)} \\ \ddot{x}_{m3(k)} \end{bmatrix} = \begin{bmatrix} z_{1(k)} \\ \left\{ \begin{array}{c} z_{9(k)}/m_2 z_{1(k)} - \frac{z_{9(k)}+z_{10(k)}}{m_2} z_{2(k)} + z_{10(k)}/m_2 z_{3(k)} + \\ z_{12(k)}/m_2 z_{5(k)} - \frac{z_{12(k)}+z_{13(k)}}{m_2} z_{6(k)} + z_{13(k)}/m_2 z_{7(k)} \end{array} \right\} \\ \left\{ \begin{array}{c} z_{10(k)}/m_3 \cdot z_2(k) - z_{10(k)}/m_3 \cdot z_{3(k)} + \\ + z_{13(k)}/m_3 z_6(k) - z_{13(k)}/m_3 z_{7(k)} \end{array} \right\} \end{bmatrix} + \tag{35}$$

$$+ \begin{bmatrix} \eta_1 \\ \eta_2 \\ \eta_3 \end{bmatrix} + \begin{bmatrix} 0 \\ F_{2(k)}/m_2 \\ F_{3(k)}/m_3 \end{bmatrix}$$

Note that the observation equations could be suitably modified in order to account for the availability of different types of sensor measurements such as strain or tilt data. The above relationships are essentially in the form presented in equations (3), (4). Thus, we can implement the previously described methods to identify the states and the parameters of the system.

5.1. Generate Measured Data

For the data simulation we chose $m_1 = m_2 = m_3 = 1, c_1 = c_2 = c_3 = 0.25, k_1 = k_2 = k_3 = 9, \beta = 2, \gamma = 1, n = 2$. The sampling frequency of the Northridge (1994) earthquake acceleration data that was used as ground excitation ($\ddot{v}_g$), is 100Hz (T=0.01 sec). The Northridge earthquake signal was filtered with a low frequency cutoff of 0.13 Hz and a high frequency cutoff of 30 Hz. (PEER Strong motion database: http://peer.berkeley.edu/smcat). A duration of 20 seconds of the earthquake record was adopted in this example. The system responses of the displacement velocity and acceleration were obtained by solving the differential equation (29), using fourth order Runge Kutta Integration, after bringing the equations into state space form:

$$\begin{bmatrix} \dot{y}_1 \\ \dot{y}_2 \\ \dot{y}_3 \\ \dot{y}_4 \\ \dot{y}_5 \\ \dot{y}_6 \\ \dot{y}_7 \end{bmatrix} = \begin{bmatrix} \dot{x}_1 \\ \dot{x}_2 \\ \dot{x}_3 \\ \dot{r}_1 \\ \ddot{x}_1 \\ \ddot{x}_2 \\ \ddot{x}_3 \end{bmatrix} = \begin{bmatrix} y_5 \\ y_6 \\ y_7 \\ y_5 - 2|y_5||y_4|^{2-1} y_4 - 1 \cdot y_5 |y_4|^2 \\ -9y_4 - 9y_1 + 9y_2 - 0.5y_5 + 0.25y_6 - \ddot{v}_g \\ 9y_1 - 18y_2 + 9y_3 + 0.25y_5 - 0.5y_6 + 0.25y_7 - \ddot{v}_g \\ 9y_2 - 9y_3 + 0.25y_6 - 0.25y_7 - \ddot{v}_g \end{bmatrix} \tag{36}$$

5.2. Simulation Results

The Unscented Kalman Filtered UKF with 33 Sigma Points (2*L+1; where L=16 is the dimension of the state vector), the Generic Particle Filter (PF) and the Sigma Point Bayes Filter (GMSPPF) were used in order to identify the parameters describing the system and the unmeasured states. The numerical analysis was done using Matlab and the ReBEL[†] toolkit. For the case of the UKF, the initial values assumed for the state variables were the following:

$$\begin{bmatrix} x_1^0 \\ x_2^0 \\ x_3^0 \\ r_1^0 \\ \dot{x}_1^0 \\ \dot{x}_2^0 \\ \dot{x}_3^0 \end{bmatrix} = \begin{bmatrix} 0 \\ 0 \\ 0 \\ 0 \\ 0 \\ 0 \\ 0 \end{bmatrix}, \begin{bmatrix} k_1^0 \\ k_2^0 \\ k_3^0 \\ c_1^0 \\ c_2^0 \\ c_3^0 \end{bmatrix} = \begin{bmatrix} 6 \\ 6 \\ 6 \\ 0.5 \\ 0.5 \\ 0.5 \end{bmatrix}, \begin{bmatrix} \beta^0 \\ \gamma^0 \\ n^0 \end{bmatrix} = \begin{bmatrix} 3 \\ 2 \\ 1 \end{bmatrix} \tag{37}$$

For the case of the particle filter analysis an initial interval needs to be defined in order to initialize the particles corresponding to the constant parameters. The interval assumed for each constant state component was:

$$\left\{k_1^0, k_2^0, k_3^0\right\} \in [4\ \ 12], \left\{c_1^0, c_2^0, c_3^0\right\} \in [0.01\ \ 1], \left\{a^0, \beta^0, n^0\right\} \in [1\ \ 5] \tag{38}$$

A study on the influence of this initial interval on the performance of the Particle Filter methods is presented later on in this section.

A random number generator was used to draw samples from the above interval. Zero mean white Gaussian noise was used for both the observation and the process noise. The process noise of 1% RMS noise-to-signal ratio was added only in the case of the state variables $z5, z6, z7$ where data from acceleration measurements are utilized. The observation noise level was of $4-7\%$ root mean square (RMS) noise to signal ratio. Based on the intervals defined for the initial conditions of the constant parameters the use of 5000 particles seemed to provide us with efficient results. A 5-Component Gaussian Mixture Model (GMM) was used for the approximation of the state posterior and a Square Root Central Difference Kalman Filter (SRCDKF) was used as the Sigma Point Kalman Filter required for the time update step, in the GMSPPF case.

In Figures 4 - 7, the results are plotted for the Unscented Kalman Filter (UKF) and the

[†]ReBel is a toolkit for Sequential Bayesian inference and can be freely downloaded from http://cslu.ece.ogi.edu/misp/rebel

Particle Filter methods (Generic Particle Filter - PF and Sigma-Point Bayes Filter - GMSPPF).

The duration for the Unscented Kalman Filter identification was 3.203 sec, for the PF identification with 5000 samples it was approximately 3200 sec, while for the GMSPPF identification with 5000 samples the elapsed time was 770 sec. The reduced duration of the GMSPPF versus the PF algorithm is due to the use of the Expectation Maximization algorithm (EM) and the use of a reduced number of mixing components in the posterior (5 component GMM).

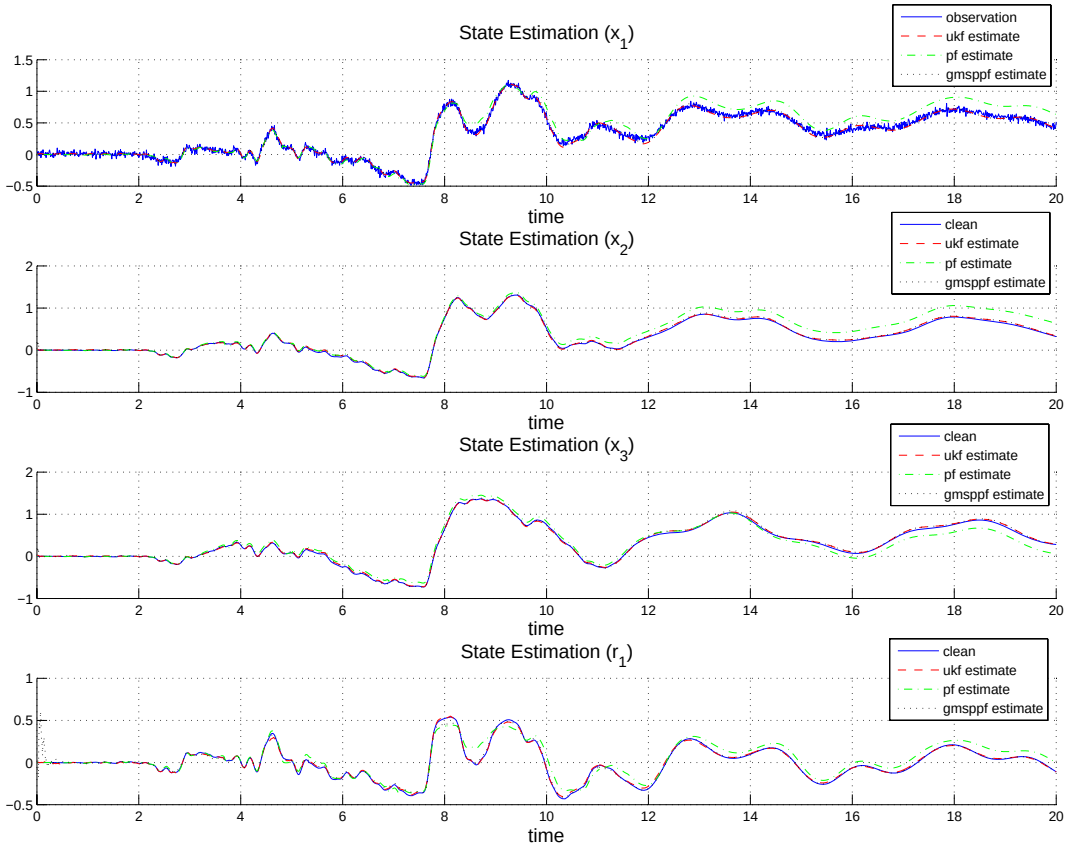

Figure 4. State Estimation Results for the UKF (dashed), standard PF (dash-dot) and GMSPPF (dotted), for the states corresponding to the displacements $x_1 : x_3$ and the hysteretic parameter r_1.

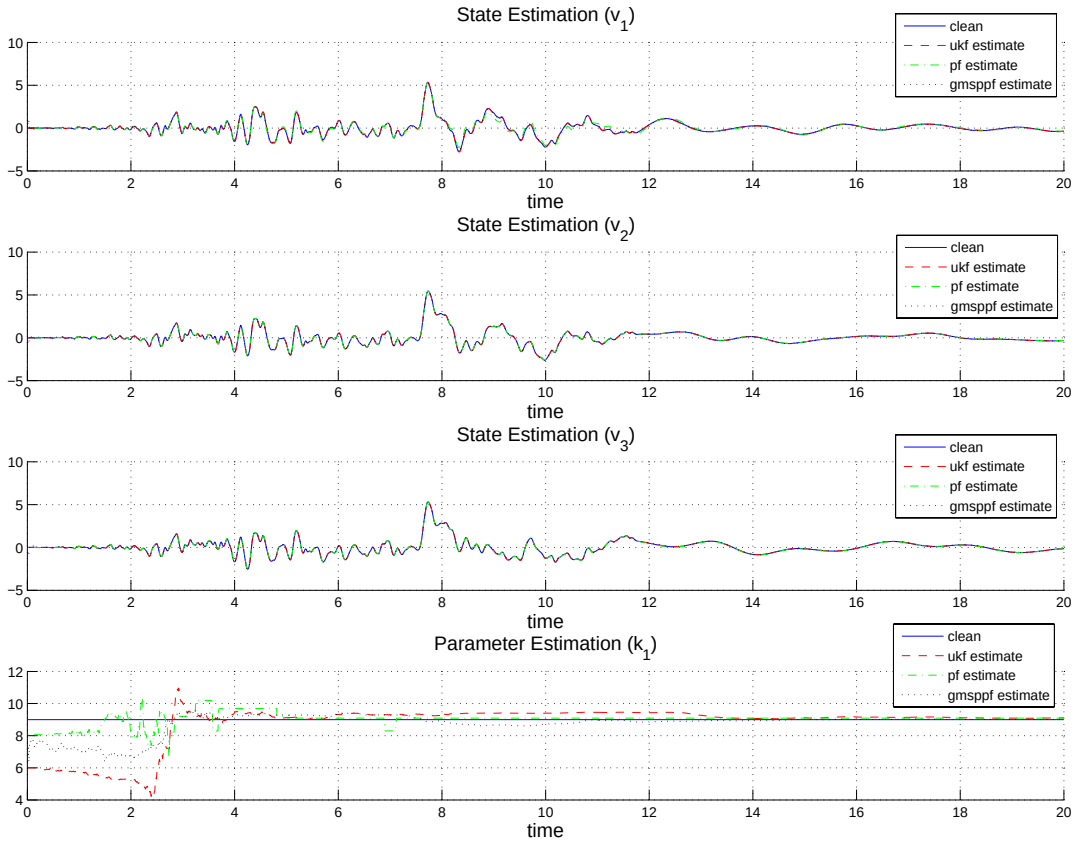

Figure 5. State Estimation Results for the UKF (dashed), standard PF (dash-dot) and GMSPPF (dotted), for the states corresponding to the velocities $v_1 : v_3$ and the stiffness parameter k_1.

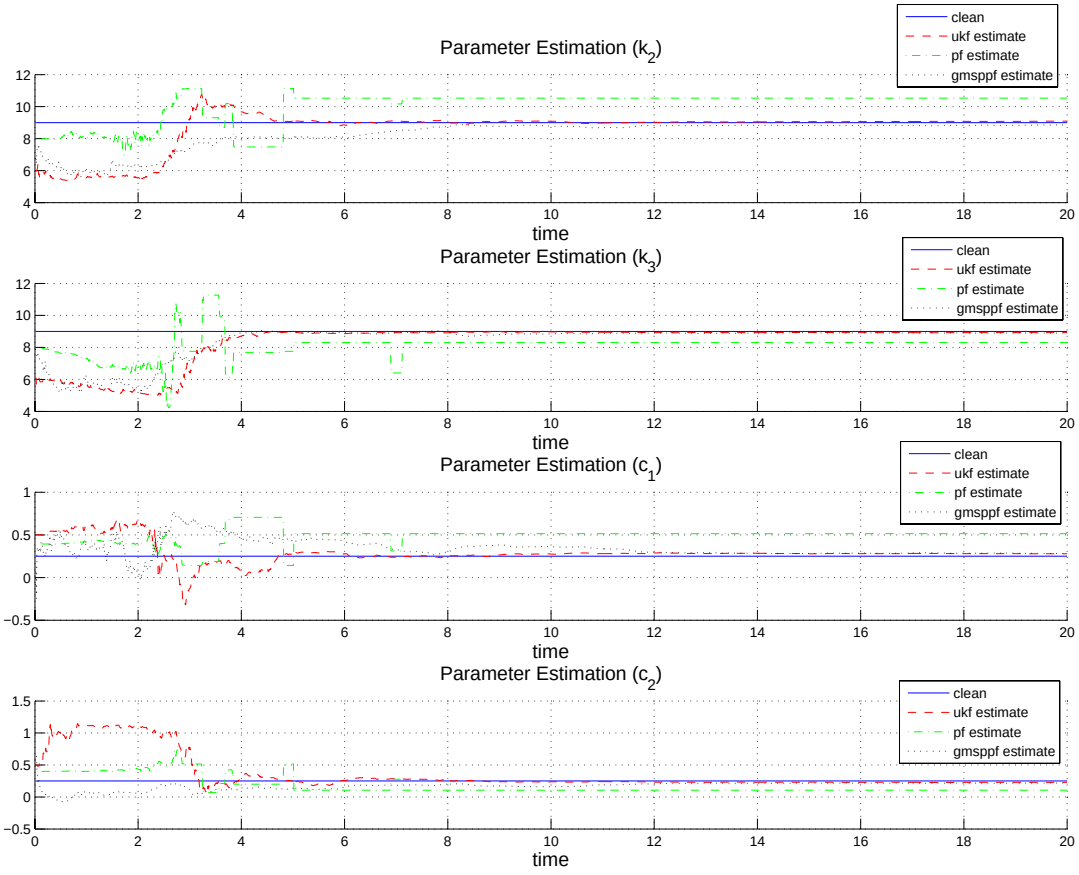

Figure 6. State Estimation Results for the UKF (dashed), standard PF (dash-dot) and GMSPPF (dotted), for the states corresponding to the stiffness parameters k_2, k_3 and the damping parameters c_1, c_2.

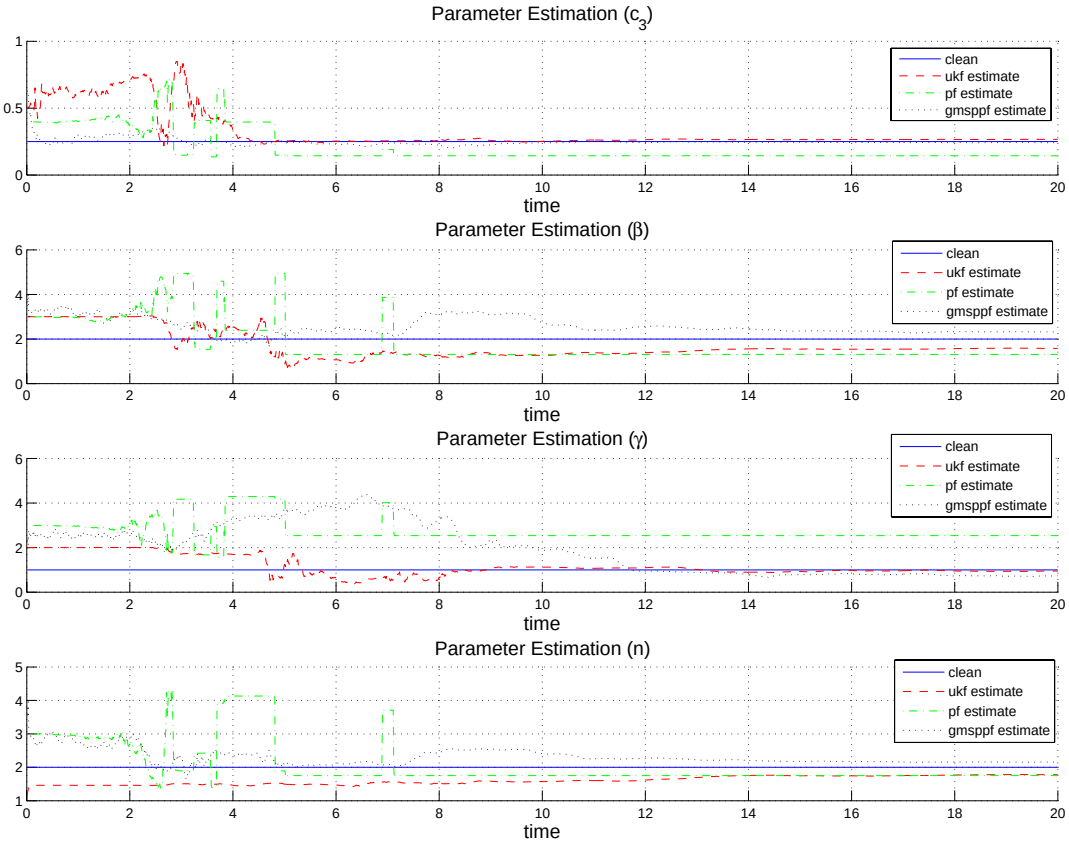

Figure 7. State Estimation Results for the UKF (dashed), standard PF (dash-dot) and GMSPPF (dotted), for the states corresponding to the damping parameter c_2 and the Bouc Wen Model parameters. α, β, n.

First of all we note the efficiency of the Unscented Kalman Filter in the estimation of the time invariant model parameters which comprise the last nine components of the augmented state vector. As Corigliano and Marani noted in [4] even though the state of the system is always followed with a high level of accuracy, the EKF can lead to unsatisfactory parameter estimations when applied to highly nonlinear behavior. This is clearly not the case for the Unscented Filter. The UKF method and the GMSPPF method provide us with very satisfactory results. Of course, as far as the computational cost is concerned the UKF method is considerably faster. On the other hand the Generic Particle Filter method, seems to be performing rather poorly and requires significantly larger computational time. The reason why the standard PF performs so badly on this problem is due first of all to the nature of the likelihood function which might lead to an initial assignment of a particularly small weight to a potentially "promising" particle. Given that the weight update in each step is dependent on the weight of the previous step, the latter prevents such promising particles from substantially influencing the weighted estimate and also leads to the promotion of other less efficient particles, leading to sample depletion through the Re-sampling process. In addition, the performance of the PF method is greatly influenced by the chosen initial condition interval. The problems of initial interval selection and sample depletion are of utmost importance in this case due to the existence of the constant states. Since, the time update in the standard Particle Filter Algorithm takes place through the process equations (34) it is obvious that time invariant state components $(z_8; z_{16})$ in each particle will remain unaltered unless at some point they are replaced by those of another particle during the Re-sampling process. The influence of the selected initial condition interval and the addition of process noise for the time invariant model parameters in order to tackle the sample depletion problem will be examined later on in this section.

Figure 8, presents a plot of the initial and final sample space for the stiffness - damping ratio pairs $(c-k)$ for each PF algorithm. As one can observe the generic Particle Filter is represented by a single sample in the final state (square point), which is the particle that survived through the Re-sampling process as the fittest. The collapse of the particle set to multiple copies of the same particle is known as the particle depletion problem, mentioned in Section 4 and it is due to the highly peaked measurement likelihood associated with the particular problem, (arising from the nature of the observation noise). On the other and, the GMSPPF maintains the variety of the sample space through the use of the Expectation Minimization (EM) algorithm, moving the particles toward areas of high likelihood.

In order to examine the effect of Re-sampling, the standard PF resampling algorithm was slightly modified so that Re-sampling only takes place if the number of efficient particles is above one third of the total number of particles. The result is plotted in Figure 9 and compared to the original PF results and the actual values. As observed in the plot, the sample space

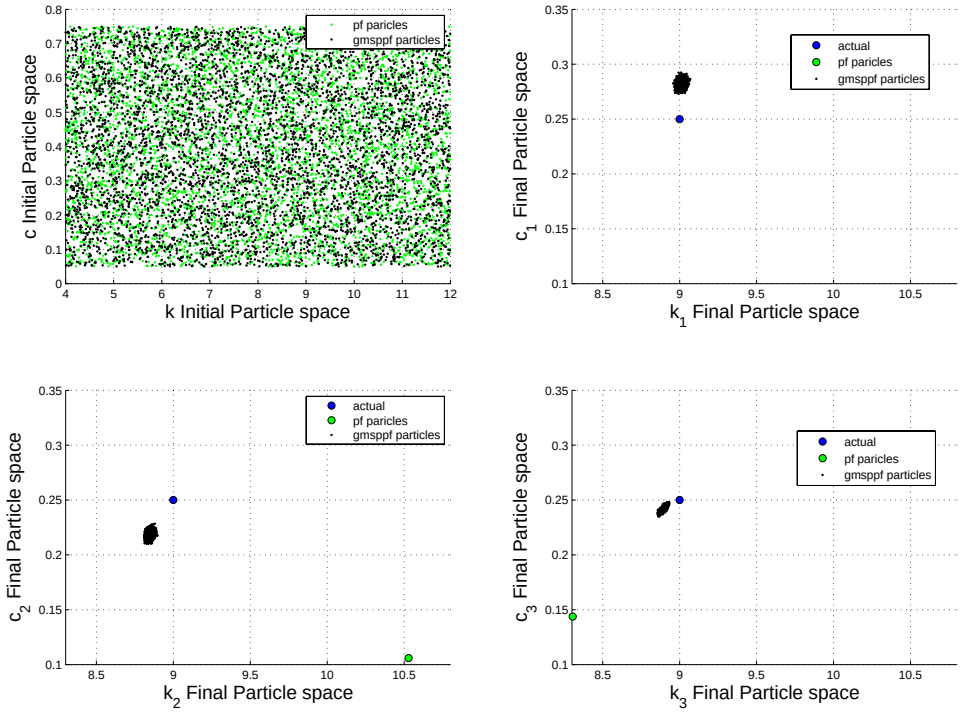

Figure 8. Representation of the Initial and Final Sample Space of the stiffness-damping parameter pairs for each Particle Filter Algorithm. The generic PF (square points) is represented by a single point in the final sample space and is evidently quite far from the actual value (circle point) compared to the GMSPPF final sample space.

for the modified PF (where the aforementioned Re-sampling constraint was added) is more varied, however the particles are not as efficiently concentrated in high likelihood areas as for the GMSPPF case (Figure 8) and the accuracy of the estimate (triangle point) is more or less around the level of the original PF estimate (square point).

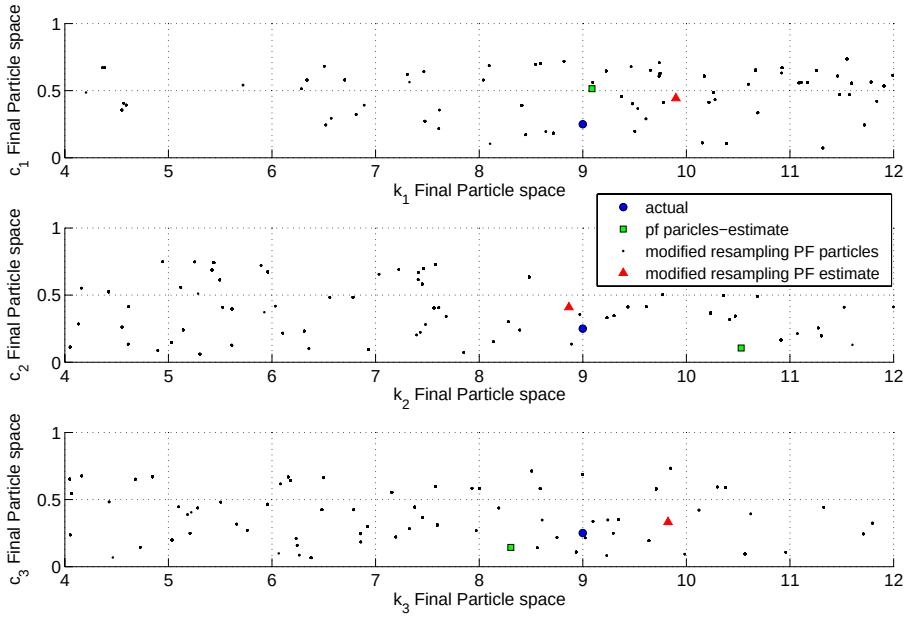

Figure 9. Representation of the Initial and Final Sample Space of the stiffness-damping parameter pairs for each Particle Filter Algorithm. The original generic PF (square point), where standard Re-sampling took place leading to the collapse of the particle set to a single component, is compared to the modified PF (black dots), where Re-sampling takes place only if the effective particles don't fall below a certain lower boundary (in order to avoid sample depletion). Although diversity is preserved in the second case the constant parameter estimate (triangle point) is not improved.

Parameter Validation

In order to assess the validity of the parameter estimation, the final values obtained from each one of the above models are used in order to recreate the response of the system (through numerical integration). Figure 10, presents the hysteretic loop generated in each case.

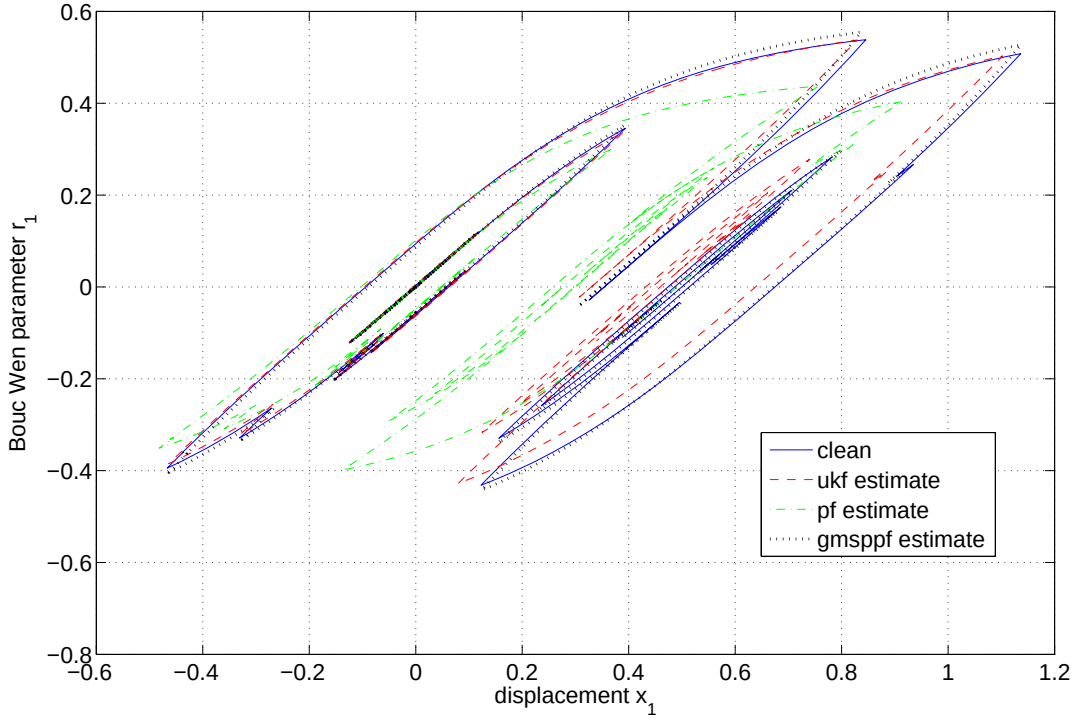

Figure 10. Parameter Validation, through the generation of the hysteretic loop for the UKF (dashed), standard PF (dash-dot) and GMSPPF (dotted)

Addition of process noise for the constant parameters

In Figures 11-12, the performance of the generic PF with 500 samples, after the addition of process noise in those components of the state equations that correspond to the time invariant model parameters (namely, z8; z16), is compared to the results obtained previously for the standard PF with more samples (5000) and no additional process noise. The additional process noise level was of approximately $0.1 - 0.5\%$ RMS (root mean square) noise to signal ratio. Results are presented for eight of the states. The response for the remaining states is similar.

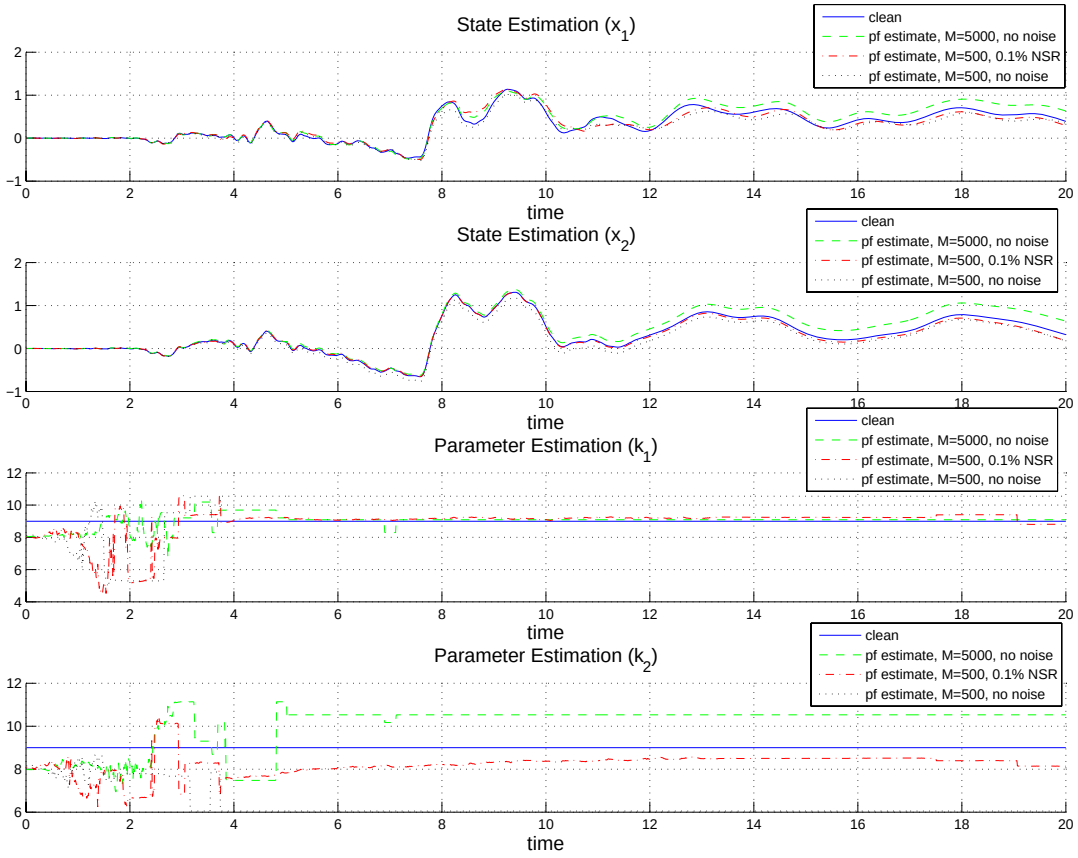

Figure 11. State Estimation Results for the standard PF-5000 samples - no additional noise (dashed), the standard PF-500 samples and additional $0.1-0.5\%$ RMS process noise for the constant parameters (dash-dot) and the standard PF-5000 samples - no additional noise (dotted).

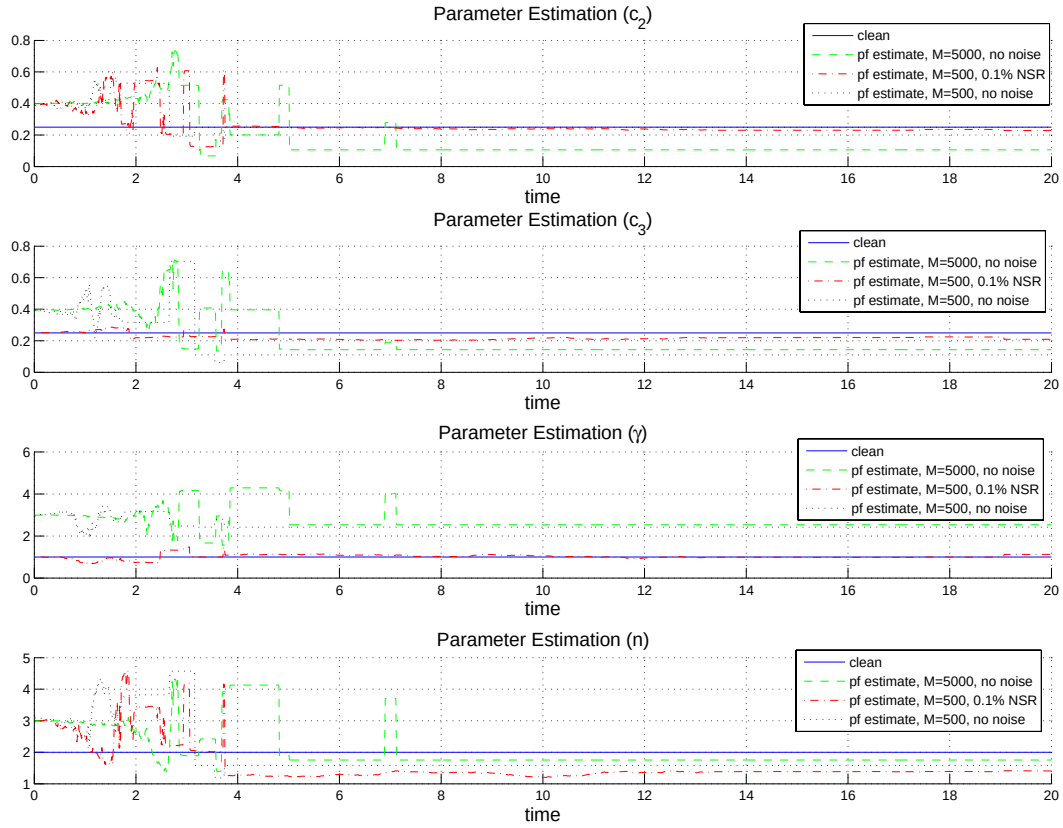

Figure 12. State Estimation results for the standard PF-5000 samples - no additional noise (dashed), the standard PF-500 samples and additional $0.1-0.5\%$ RMS process noise for the constant parameters (dash-dot) and the standard PF-5000 samples - no additional noise (dotted). The addition of a low percentage of noise for the constant parameters helped improve the standard PF behavior.

As can be inferred from the results plotted above the addition of process noise in the constant parameter state equations can potentially result in similar or even improved results compared to those obtained for a run involving a significantly larger number of particles. The time needed for the 500 particle case was approximately 40 sec which is almost one hundredth of the analysis time corresponding to the 5000 particle case. ($\propto N^2$). In addition a plot of another run of 500 samples again where no additional process noise was utilized this time is presented, where it is obvious that the accuracy of the simulation is less satisfactory compared to both the previous cases.

Influence of the Initial Condition Interval Selection for the PF

The selection of the initial condition intervals plays an important role in the efficiency of the standard PF method. The same does not apply for the GMSPPF method were the particles are fitted in a fewer component GMM. Figures 13 - 14, compare the performance of the standard PF for two additional interval choices. 1000 particles were used in both cases. The initial interval defined previously in equation (38), is a relatively wide interval containing the actual values of the constant parameters. Interval 1 is a narrower interval again containing the actual constant parameter values and finally interval 2 is a somewhat narrow interval, sufficiently close to the actual values of the initial conditions but not containing them:

$$\begin{aligned} \text{Interval1} : \{\mathrm{k_i}\} \in \begin{bmatrix} 7 & 11 \end{bmatrix}, \{\mathrm{k_i}\} \in \begin{bmatrix} 0.15 & 0.4 \end{bmatrix}, \{\alpha,\beta,n\} \in \begin{bmatrix} 1 & 5 \end{bmatrix} \\ \text{Interval2} : \{\mathrm{k_i}\} \in \begin{bmatrix} 3 & 7 \end{bmatrix}, \{\mathrm{k_i}\} \in \begin{bmatrix} 0.35 & 0.75 \end{bmatrix}, \{\alpha,\beta,n\} \in \begin{bmatrix} 2.5 & 4 \end{bmatrix} \end{aligned} \tag{39}$$

According to Figures 13-14, the standard PF performs much better given a more precise initial condition interval, however if that initial choice does not contain the correct constant parameter values (in case there is not sufficient knowledge of the model) the standard PF does not have the ability to evolve the constant states beyond the boundaries of the initial conditions interval. The addition of some process noise could help overcome this problem. In contrast, the GMSPPF does not present the same problem due to use of the GMM and the SRCDKF based time update step. This provides the GMSPPF method with the potential of varying the values for the time invariant particle components without the addition of process noise.

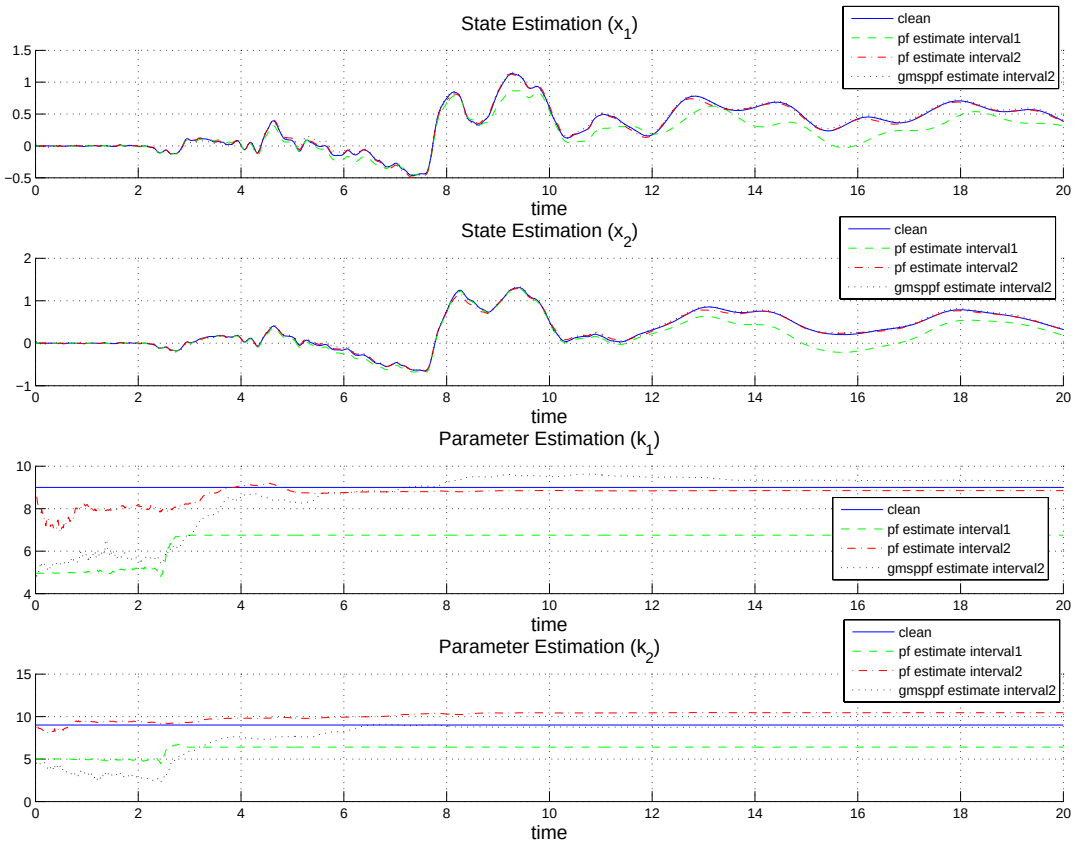

Figure 13. State Estimation Results for the standard PF for different initial conditions intervals, interval 1 (dashed) is a narrow interval containing the actual parameter values, interval 2 (dash-dot) is an interval not containing the actual values. The GMSPPF response is also plotted (dotted)

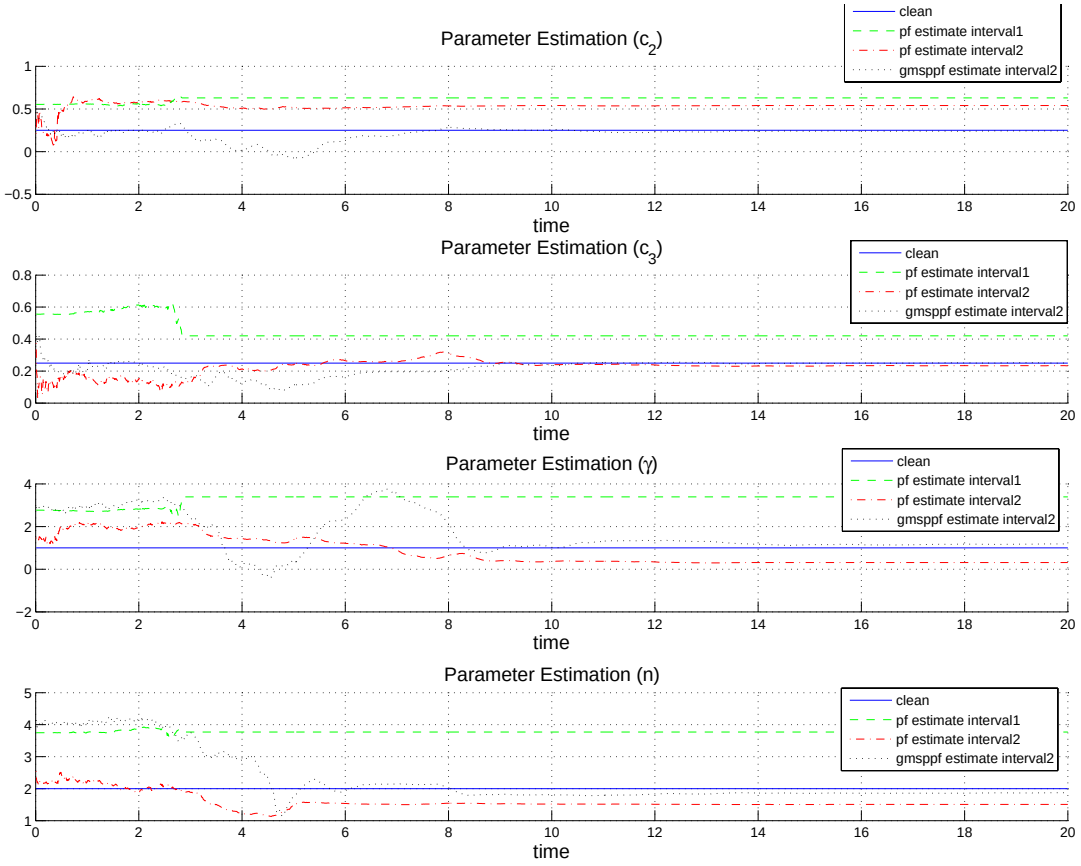

Figure 14. State Estimation Results for the standard PF for different initial conditions intervals, interval 1 (dashed) is a narrow interval containing the actual parameter values, interval 2 (dash-dot) is an interval not containing the actual values. The standard PF performs well for interval 1, however it is unable to estimate parameters outside interval 2. The GMSPPF (dotted) on the other hand is not influenced by the choice of interval2.

5.3. Importance of the Displacement Measurements

In order to highlight the importance of including displacement sensing in our identification scheme for this nonlinear structure, it is interesting to contrast the identification and state estimation results with those obtained through the use of acceleration measurements alone from each DOF. The displacement time history comparison for the two simulations is displayed in Figure 15. Results are presented for the UKF method, which is one of the two most robust techniques presented herein, so that the comparison could be clearer as to the effect of the different measurements.

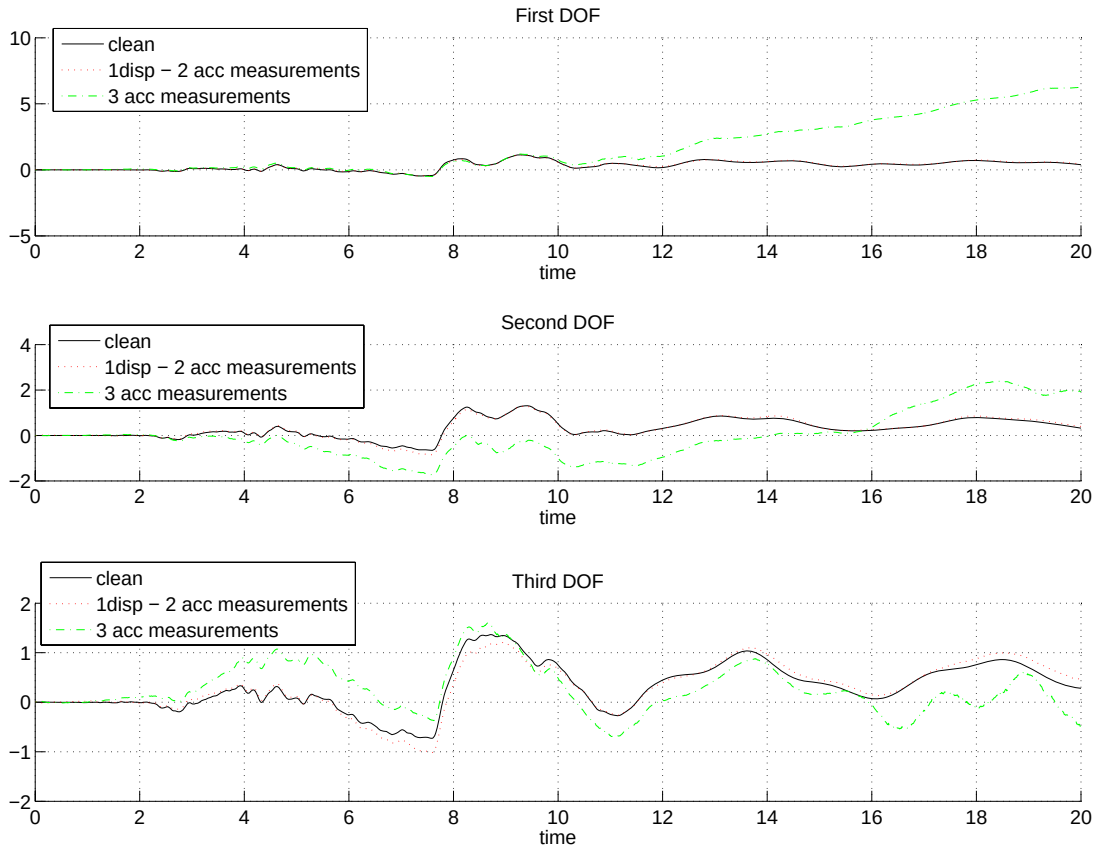

Figure 15. Displacement time history plots for the actual data (solid), the original measurement configuration simulation involving one displacement measurement (dashed) and the new measurement configuration involving solely acceleration measurements for all three DOFs (dash dot)

As observed in Figure 15, the state estimation especially in the case of the first degree of freedom -which is associated with a non-linear hysteretic component- is significantly improved in the case where displacement data is available. Hence, it can be said that the availability of displacement measurements is immensely beneficial for the accurate rapid identification of nonlinear systems such as the one presented herein where the state equations are functions of displacement and velocity.

6. CONCLUSIONS

A comparison of the use of two PF based methods and the UKF method is shown for the adaptive estimation of both unmeasured states as well as invariant model parameters. This general class of method was adopted to tackle the problem due to the nonlinear nature of the physical system as well as the nonlinearity in the measurement equations introduced by the non collocated displacement and acceleration measurements. Although, the UKF was the most computationally efficient, in fact with the potential of running in real time, the GMSPPF technique was more robust.

For the example considered, the UKF and GMSPPF techniques proved to be the most efficient ones when performing a validation comparison using the final identified parameters, with the GMSPPF method proving to be the most accurate one especially when it comes to the estimation of time invariant model parameters. The performance of the PF method, which proved to be less accurate than the two aforementioned ones, can be improved through the addition of some artificial process noise, corresponding to the time invariant model parameters, as this helps overcome the sample depletion problem. In fact, the latter led to improved PF estimates even when using a lesser number of particles. Also, without the addition of artificial process noise the generic PF method was shown to perform poorly in identifying the time invariant model parameters if the initial interval from which the particles were sampled did not contain the true value of the corresponding parameters. As shown in section 5.2 the precision in the definition of the initial interval holds an important role in the convergence of the standard PF algorithm. For the Gaussian Mixture Particle Filter method (GMSPPF) on the other hand, the particles themselves evolve and therefore it is not an intrinsic problem for the true value of the constant parameters to lie outside the initial interval. In addition, the influence of the availability of displacement measurements has been explored leading, not surprisingly, to the deduction that it is indeed of utmost importance for the identification of states related to nonlinear functions of displacement. As seen from (30) this is the case for the first degree of freedom of the application presented herein.

Future work will explore robustness to measurement noise as well as the identifiability

limitations of the method as the system complexity increases and the number of sensors decreases. In addition, a variation of the Re-sampling process for the generic PF will be investigated, where instead of multiplying the fittest samples and eliminating the weakest ones, a Genetic Algorithm approach will be implemented where new samples (children) are reproduced from the fittest ones (parents), in order to replace those with negligible weights.

ACKNOWLEDGMENTS

This study was supported in part by the National Science Foundation under CAREER Award CMS-0134333. In addition, the second author would like to acknowledge the support of the Laboratoire Central des Ponts et Chaussées where he was visiting when this study began.

REFERENCES

1. A. W. Smyth, S. F. Masri, A. G. Chassiakos, T. K. Caughey, On-line parametric identification of mdof nonlinear hysteretic systems, Journal of Engineering Mechanics 125 (2) (1999) 133–142.
2. A. W. Smyth, S. F. Masri, E. B. Kosmatopoulos, A. G. Chassiakos, T. K. Caughey, Development of adaptive modeling techniques for non-linear hysteretic systems, International Journal of Non-Linear Mechanics 37 (8) (2002) 1435–1451.
3. Y. CB, S. M., Identification of nonlinear structural dynamics systems, Journal of Structural Mechanics 8(2) (1980) 187–203.
4. A. Corigliano, S. Mariani, Parameter identification in explicit structural dynamics: performance of the extended kalman filter, Computer Methods in Applied Mechanics and Engineering 193 (36-38) (2004) 3807–3835.
5. S. Mariani, A. Corigliano, Impact induced composite delamination: state and parameter identification via joint and dual extended kalman filters, Computer Methods in Applied Mechanics and Engineering 194 (50-52) (2005) 5242–5272.
6. S. J. Julier, J. K. Uhlmann, A new extension of the kalman filter to nonlinear systems., Proceedings of AeroSense: The 11th Int. Symposium on Aerospace/Defense Sensing, Simulation and Controls.
7. E. Wan, R. Van Der Merwe, The unscented kalman filter for nonlinear estimation, in: Adaptive Systems for Signal Processing, Communications, and Control Symposium 2000. AS-SPCC. The IEEE 2000, 2000, pp. 153–158.
8. T. Chen, J. Morris, E. Martin, Particle filters for state and parameter estimation in batch processes, Journal of Process Control 15 (6) (2005) 665–673.
9. J. Ching, J. L. Beck, K. A. Porter, R. Shaikhutdinov, Bayesian state estimation method for nonlinear systems and its application to recorded seismic response, Journal of Engineering Mechanics 132 (4) (2006) 396–410.
10. S. Arulampalam, S. Maskell, N. Gordon, T. Clapp, A tutorial on particle filters for on-line non-linear/non-gaussian bayesian tracking, IEEE Transactions on Signal Processing 50 (2) (2002) 174–188.
11. J. L. B. Jianye Ching, K. A. P. Keith A. Porter, Bayesian state and parameter estimation of uncertain dynamical systems, Probabilistic Engineering Mechanics 21 (2006) 81-96.
12. J. N. Yang, S. Lin, H. Huang, L. Zhou, An adaptive extended kalman filter for structural damage identification, Structural Control and Health Monitoring 13 (4) (2006) 849–867.

13. H. Zhang, G. C. Foliente, Y. Yang, F. Ma, Parameter identification of inelastic structures under dynamic loads, Earthquake Engineering & Structural Dynamics 31 (5) (2002) 1113–1130.
14. S. Mariani, A. Ghisi, Unscented kalman filtering for nonlinear structural dynamics, Nonlinear Dynamics 49 (1) (2007) 131–150.
15. M. Wu, A. W. Smyth, Application of the unscented kalman filter for real-time nonlinear structural system identification, Journal of Structural Control and Monitoring 14, No. 7 (November. 2007) 971–990.
16. N. G. B. Ristic, S. Arulampalam, Beyond the Kalman Filter, Particle Filters for Tracking Applications, Artech House Publishers, 2004.
17. N. Bergman, Recursive bayesian estimation: Navigation and tracking applications, Ph.D. thesis, Linkoping University, Sweden (1999).
18. N. Bergman, A. Doucet, N. Gordon, Optimal estimation and cramer rao bounds for partial non gaussian state space models, Ann. Inst. Statist. Math. 53(1) (2001) 97–112.
19. R. van der Merwe, E. Wan, Gaussian mixture sigma-point particle filters for sequential probabilistic inference in dynamic state-space models.
20. S. J. Ghosh, C. Manohar, D. Roy, A sequential importance sampling filter with a new proposal distribution for state and parameter estimation of nonlinear dynamical systems, Proceedings of the Royal Society A: Mathematical, Physical and Engineering Sciences 464 (2089) (2008) 25–47.
21. A. Doucet, C. Andrieu, Particle filtering for partially observed gaussian state space models (CUED/FINFENG /TR393).
22. N. Kwok, G. Fang, W. Zhou, Evolutionary particle filter: re-sampling from the genetic algorithm perspective, Intelligent Robots and Systems, 2005. (IROS 2005). 2005 IEEE/RSJ International Conference on (2005) 2935–2940.
23. G. Zhu, D. Liang, Y. Liu, Q. Huang, W. Gao, Improving particle filter with support vector regression for efficient visual tracking, Image Processing, 2005. ICIP 2005. IEEE International Conference on 2 (2005) II–422–5.